CONF-9505266--1

SAND95-1669C

The Shoemaker-Levy 9 Impact Plumes on Jupiter: Implications for Threat to Satellites in Low-Earth Orbit

M. B. Boslough and D. A. Crawford
Sandia National Laboratories

Computational simulations of the impacts of comet Shoemaker-Levy 9 (SL9) fragments on Jupiter have provided a framework for interpreting the observations. A reasonably consistent picture has emerged, along with a more detailed understanding of atmospheric collisional processes. Several aspects of Earth-impact hazards can be re-evaluated with knowledge gained from observations and from simulations of SL9. In particular, the threat of impact-generated plumes to satellites in low-Earth orbit (LEO) should be recognized. Preliminary 2-D computational simulations suggest that impacts of a size that recur about once per century generate plumes that rise to nearly 1000 kilometers over an area thousands of kilometers in diameter. Detailed modeling of such plumes should be carried out to quantify this threat to satellites in the near-Earth environment. Careful observations of high-energy atmospheric entry events should be made using both satellite and ground-based instruments to provide validation for these computational models.

Introduction

The multiple impacts of comet SL9 fragments with Jupiter in July 1994 provided an historic opportunity to directly observe the phenomena resulting from hypervelocity collisions on a planet. Detailed analysis of this event has advanced our understanding of comets, of Jupiter, and of the collisional processes that shaped the solar system. This improved understanding can now be used develop better models for the assessment of the impact threat to Earth.

The principal reason we performed computational simulations of the SL9 impacts was to take advantage of a "natural experiment" to validate Sandia's shock physics codes, CTH and PCTH (McGlaun et al., 1990), for an impact involving velocities, masses, and kinetic energies many orders of magnitude higher than had ever before been witnessed. By simulating a natural astronomical event, the validation could be based on observational, rather than on experimental data. Additional reasons for our work were to 1) provide predictions to help guide astronomical observations of the event, and 2) assist astronomers in interpreting the observational data.

Prior to impact, the computational effort was focused primarily on making predictions. In the period between the recognition (in mid-1993) that SL9 would strike Jupiter, and the availability (in early 1994) of new astrometric data, the estimated point of impact was far on Jupiter's back side, and there was little hope for a direct view from Earth. After better orbital data put the impact point about six degrees over the Jovian limb, more attention was focused on the fireball/plume phenomena that had the greatest potential for being observable. By the time the comet arrived at Jupiter, there was general agreement among the impact modeling groups that, for sufficiently large impactors, debris ejected by the collisions would rise into line of sight of Earth (Zahnle and Mac Low, 1994; Stellingwerf et al., 1994; Ahrens et al., 1994; Boslough et al., 1994a,b; Shoemaker et al., 1995).

The fireballs and plumes predicted by the models were indeed observed, but the actual event produced a much richer array of consequences than anyone anticipated. Because of a massive international effort, an overwhelming amount of high-quality observational data was collected during impact week. Some of the new phenomena have already been explained and are fully consistent with the models. Interpretation of other observations will require further analysis and synthesis of the data. We expect that computational modeling will continue to provide guidance and contribute to our understanding of this event. Moreover, the simulations--coupled with observational results of the SL9 impact--will enhance our ability to predict the consequences of an comet or asteroid impact on Earth, leading to improved threat assessments. The purpose of this paper is to summarize a "big picture" interpretation that is consistent with much of the observational data that has become available to date (see: *Science, 267*, March 3, 1995, *Geophys. Res. Lett. 22(12)*, June 15, 1995, *Science 268*, June 30, 1995, and *Geophys. Res. Lett. 22(13)*, July 1, 1995), and to point out implications for impact hazard assessment on Earth.

MASTER

DISCLAIMER

Portions of this document may be illegible
in electronic image products. Images are
produced from the best available original
document.

SL9 observations

The geometry and timing of the series of impacts could hardly have been better for making useful observations from Earth (Figure 1). With the impact location only a few degrees beyond Jupiter's limb, the hot debris ejected by each collision had to rise only a few hundred kilometers to become visible. It could then be seen in profile, making it possible to observe its shape and size. The vantage point from Earth was close to perpendicular to the trajectory of the fragments, so that the effect of impact obliquity could be seen. Because the impact point was beyond the limb (horizon), the time of arrival of debris above the line-of-sight altitude could be measured. Combining this information with the time of impact extracted from direct measurements from Galileo (and in some cases from Earth), the fireball trajectory can be determined. The position of Jupiter (near quadrature) put the luminous debris in shadow when it first
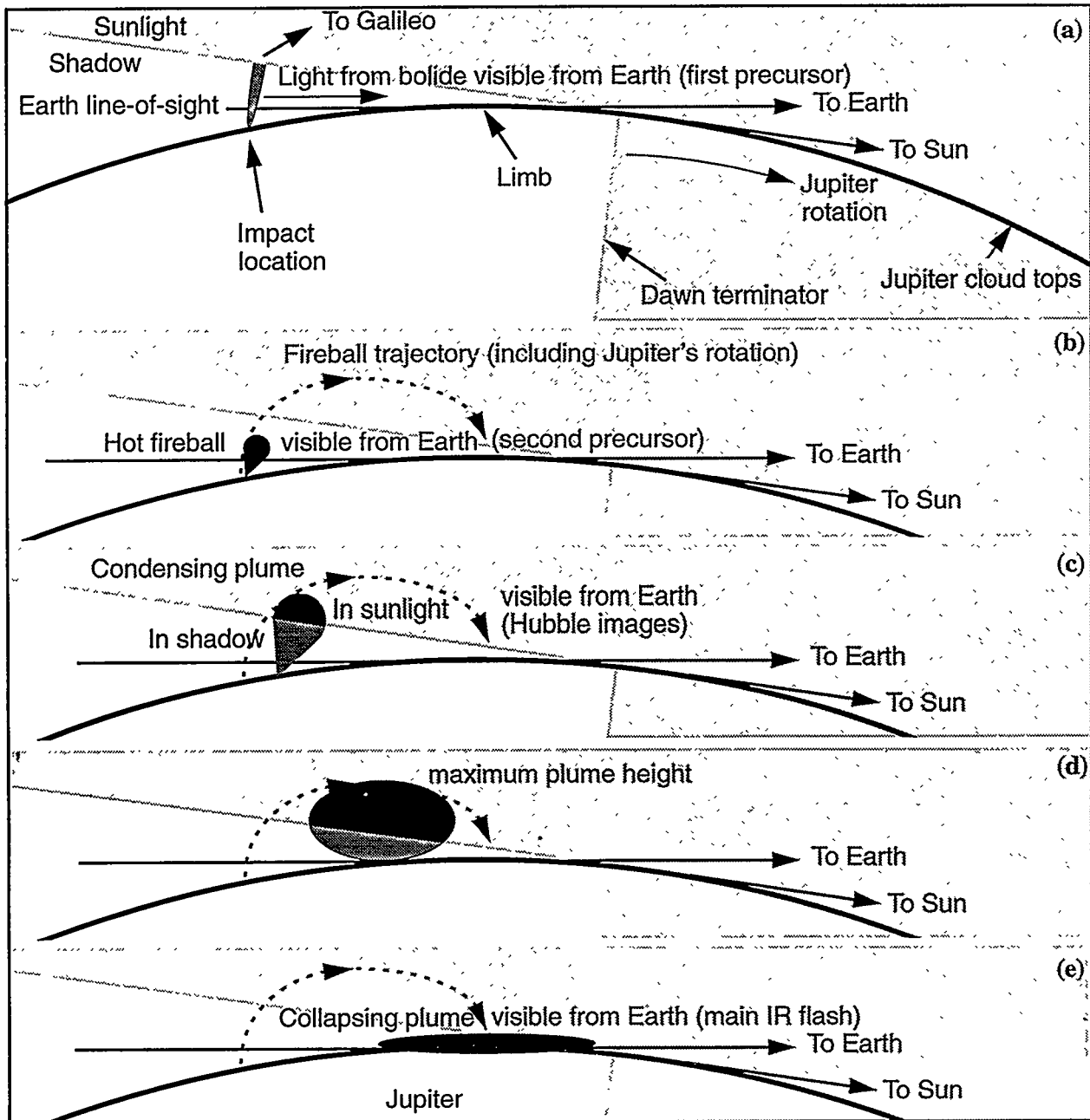

Figure 1. Geometry of impacts, just beyond Jupiter's limb (horizon) as viewed from Earth; (a) Dust and main fragment enter Jupiter's atmosphere, generating entry flash, (b) Incandescent fireball rises into view from Earth, (c) condensing plume ballistically rises into sunlight, (d) Plume reaches maximum altitude of about 3300 km above clouds, (e) Plume collapses and rotates into view (modified from Boslough et al., 1994b)

rose into view, making it possible to determine its brightness. This configuration also means that additional trajectory information can, in principle, come from the time of arrival of the fireball into sunlight. Morphology information can be extracted from the shadow-line on the plume. Furthermore, each impact site was on the side of Jupiter (near local dawn) that immediately rotated into view from Earth, giving the fireball a velocity component toward the limb, and making it possible to observe the pattern of debris and wave phenomena immediately after impact. This best-case impact configuration allows many direct comparisons to be made between simulations and observations.

The event took place at a time that was extremely fortuitous in terms of the instruments that could be used to make observations of the impact sites. The Hubble Space Telescope (HST) and the Galileo spacecraft were both available to complement Earth-based observations. HST happened to be in position to directly image the plumes from four impacts, and Galileo had a direct line of sight for all the impacts. HST images have provided information about the size, shape, evolution, and optical properties of the fireballs and plumes, and about the structure and evolution of the impact sites after plume collapse (Hammel et al., 1995). HST and Earth-based spectroscopy yielded evidence for water, ammonia, iron, silicon, magnesium, sodium, calcium, lithium, potassium, diatomic sulfur other sulfur compounds, carbon monoxide, and hydrogen cyanide at the impact sites (Noll et al., 1995, Bjoraker et al., 1994; Yelle et al., 1994; Maillard et al., 1995; Marten et al., 1995; Roos-Serote et al., 1995). Galileo has provided precise timing for the entry of many of the fragments into the atmosphere, as well as information about the expansion rates and cooling histories of the incandescent fireballs (Martin et al., 1995; Carlson et al., 1995; Chapman et al., 1995, Hord et al., 1995). The event timing as determined by Galileo measurements has provided a strong basis for interpreting the multiple flashes observed from Earth in a way that is consistent with the computational models (Figure 2)

We use the term "fireball" to refer to the mass of hot gases consisting of a mixture of Jovian atmosphere and cometary material that is ballistically shot upward by the impact. In the first moments after impact it is very hot, incandescent, and radiating in the visible and near infrared. The fireball is preceded by the "entry flash" or "bolide" phase, during which time the comet fragment (and associated debris) deposits its energy in Jupiter's atmosphere. The entry flash as seem from Earth may be dominated by the deposition of energy at very high altitude (above the limb) by small particles in the coma surrounding the main fragment, and for that reason its use as a timing fiducial may not be straightforward. The main fragment mass does not begin to deposit a large amount of energy until it has passed beyond the limb, after which it begins to heat an entry column of atmosphere as it loses its kinetic energy. It is that column of gas that explosively expands and becomes the fireball. We use the word "plume" to describe the debris cloud after it has expanded, cooled adiabatically, and begun to condense. Clearly, there are no precise temporal demarcations separating bolide, fireball, and plume phases.
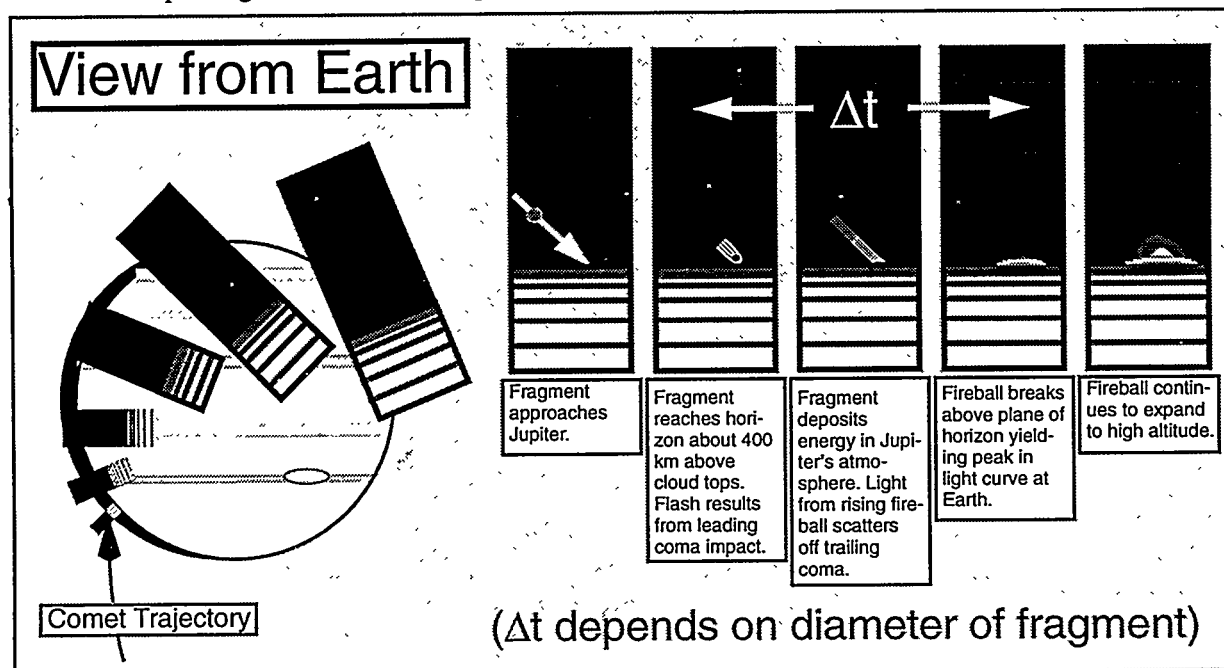

Figure 2 Cartoon representation of early part of impact/fireball sequence as seen from Earth, with method of constraining initial fireball trajectory. In reality, entry flash and fireball arrival times are blurred by dust and indirect light scattering.

SL9 interpretations

Figures 3 and 4 depict idealized schematic representations of the sequence of events inferred from Earth-based photometry data, Galileo light curves, and HST imagery. Figure 3 is a plan view of the impact site from a stationary (non-rotating) vantage point, with snapshots of a map projection of the evolving impact sites at various time steps after impact. As the point of impact rotates from west to east, it moves from left to right in the stationary field of view of the illustration. Jovian north is up; the approximately vertical lines represent the minimum line-of-sight altitudes to the Earth and sun. The figure is not intended to depict the exact geometry, nor is it supposed to represent a particular impact, but is a composite of features observed from various events. Figure 4 shows a simplified side view of the fire-ball/plume evolution. In reality, the ejecta cloud is not a discrete packet but a continuum with widely varying temperatures, densities, and pressures. In addition, the impacts were not necessarily the "clean experiments" described here, but probably involved closely-spaced multiple impactors embedded within a dusty, light-scattering cloud of smaller particles (coma), which also had a hypervelocity, light-producing interaction with Jupiter's atmosphere.

In the Figure 3 inset are some idealized examples of Galileo and Earth-based light curves. The Galileo Photopolarimeter Radiometer (PPR) curve is based on the measurements of several impacts at 945 nm (Martin et al., 1995). The upper Earth-based light curve resembles data at 3.5 μm collected at the Palomar Observatory by Nicholson et al. (1994) for the R impact; a similar curve was obtained by Graham et al. (1994) at 2.3 μm with the Keck Telescope, and for the K impact at 2.35 μm at the Okayama Astrophysical Observatory by Takeuchi et al. (1995). The lower curve is based on 10 μm data collected at the European Southern Observatory by Livengood et al. (1994).

The following is a description of the sequence of events, with letters corresponding to those in Figures 3 and 4. The various phases are defined primarily for conceptual purposes; there are not distinct demarcations between them, and in many cases they overlap. Approximate times relative to initial entry are listed for each phase.
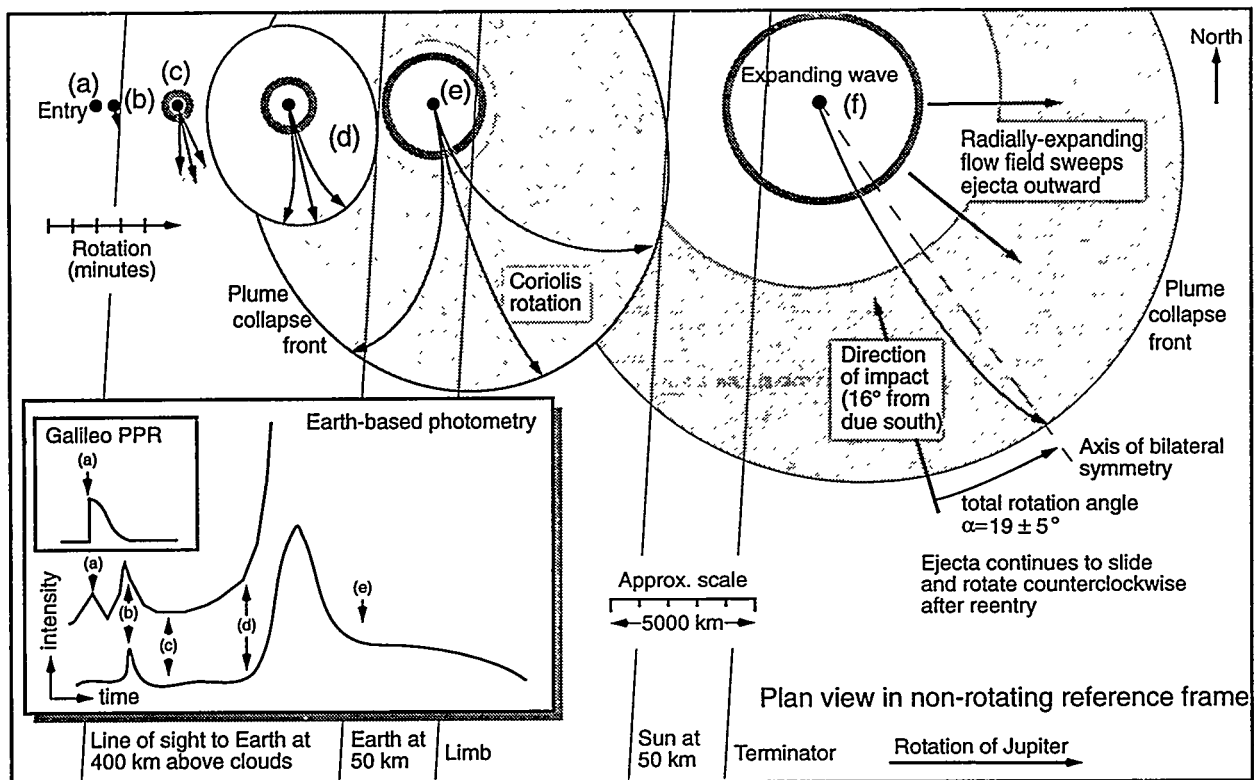

Figure 3 Plan view (map projection) of idealized impact site from a stationary (non-rotating) vantage point, with snapshots of a planar projection of its evolution, interpreted using the conceptual framework provided by computational simulations. This figure schematically represents features that were seen after several of the larger impacts. See text for detailed explanation (from Boslough et al., 1995).

4

(a) Entry phase (zero to 10 or 15 seconds)

A fragment (or cluster) enters Jupiter's atmosphere, depositing energy and leaving a debris column that consists of a mixture of Jovian atmosphere and cometary vapor at high temperatures and pressures. Thermal radiation from this column is seen directly by Galileo's instruments, and, for some impacts, via scattered light (or directly in the earliest stages) from Earth. This appears as the first precursor in some of the Earth-based light curves. The long risetime associated with this precursor is probably due to the direct view from Earth of the hypervelocity collision of the leading part of the coma into Jupiter's upper atmosphere.

(b) Fireball phase (5 or 10 seconds to 3 or 4 minutes)

The column explosively expands upward and outward along the atmospheric density gradient, cooling isentropically as it rises. The expansion begins instantaneously, before the entry phase is complete. This is seen by Galileo as a decrease in radiative intensity, and a shift toward longer wavelengths in thermal emission. Within one minute, the incandescent fireball rises to a few hundred kilometers and becomes visible from Earth, appearing as another precursor in photometry data. The exact timing depends on both fragment size and the point of impact, as summarized by Crawford et al. (1995). The fireball is preceded by several seconds by a shock wave. Earth-based detection of this shock would provide strong validation of the computational models, but it may be too weak to have been seen as an independent precursor. The arrival time of hot material above the Jovian limb, as viewed from Earth, is probably blurred by fireball light scattered from trailing coma material.

(c) Plume phase (3 or 4 minutes to 10 or 15 minutes)

The debris continues to rise ballistically. It expands and cools, and begins to condense. When it reaches an altitude greater that one or two thousand kilometers (depending on the point of impact), it enters sunlight. Careful analysis of time-resolved photometry might provide the timing for this event, which would be useful for reconstructing the ballistic trajectory.

(d) Maximum height (between about 6 and 9 minutes)

The lower part of the debris cloud begins to collapse and heat Jupiter's stratosphere. As the front of this heated region propagates and rotates over the limb, the strongest peak in the Earth-based light intensity curves begins to appear.

(e) Plume collapse phase (about 5 to 15 minutes)

As the still-expanding debris cloud begins to fall back, it compresses and heats a large area of the Jovian stratosphere. The heated region grows rapidly. The peak in Earth-based photometry curves is determined by a combination of competing effects, including increasing area, radiative and decompressional cooling, and viewing geometry.
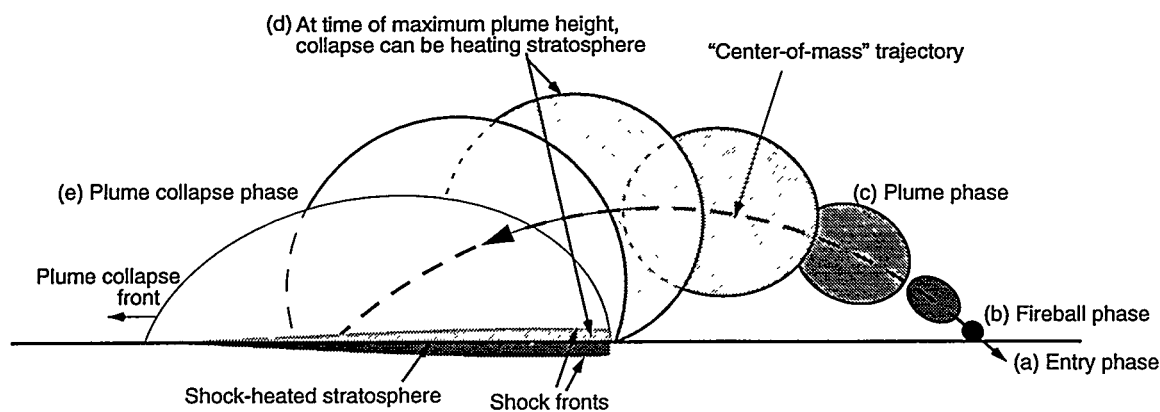

Figure 4. Side view of highly idealized fireball/plume evolution which leads to a "hypervelocity splat" when the plume collapses, heating Jupiter's upper atmosphere over a very large area. This schematic shows the ejecta cloud as a discrete packet, rather than the continuum it really is (modified from Boslough et al., 1995).

Recently-downloaded data on the R impact from Galileo's Near Infrared Mapping Spectrometer (NIMS) has now provided direct evidence for stratospheric heating from the collapse of the plume, and timing information for that event (Carlson et al., 1995). The expanding debris cloud rotates counterclockwise due to the Coriolis Effect, so the ejecta footprint's symmetry axis does not line up with the fragment trajectory. The outwardly-directed velocity component sets up a radially-expanding flow field that sweeps condensed matter outward.

(f) Post-collapse "splat" phase (about 15 to 45 minutes)

The plume collapse goes to completion. The fully-collapsed ejecta blanket continues to expand radially and rotate counter-clockwise until stopped by viscous and other dissipative forces. The final angle between the impact trajectory and axis of bilateral symmetry depends on how much rotation takes place after the plume collapses. The post-collapse rotation is evidence that ejected material flows horizontally over very long distances after reentry, and indicates that the ejecta blanket also expanded radially. A linear, radially expanding wave is made visible by an unknown mechanism, possibly condensation in the rarefaction part of the wave.

(g) Upwelling phase (minutes to hours)

The computational models indicate that there is also an upwelling phase. Careful examination of the 3-D simulations of Crawford et al. (1995) reveals that for massive, deeply-penetrating impactors, a bubble (or several bubbles) of hot Jovian atmosphere mixed with cometary vapor rises buoyantly from the depth of maximum energy deposition. This is between 200 and 300 km beneath the 1 bar level for 2-3 km diameter fragments. At 82 seconds after impact for a 1-km impactor there are three or four instabilities developing between about 50 and 200 km below the 1 bar level. At this time, they are 20-30 km in diameter, and have risen by about that distance from their starting point. These bubbles are analogous to buoyant nuclear explosion fireballs. Extrapolation of their upward motion suggests that they will begin arriving at the ammonia cloud layer within minutes, after having adiabatically expanded to many times their size. The resulting massive displacement of atmosphere is a likely source for the expanding wave. The upwelling might also manifest itself as thermal brightening or appearance of new spectroscopic signatures at the impact sites. It may be possible to extract information about the penetration depth (and therefore fragment mass) from the timing, temperature, and composition of any buoyantly-upwelling material. High-resolution 3-D simulations of this buoyancy phase are clearly needed.

SL9 computational simulations

Crawford et al. (1995) used the CTH Eulerian shock-physics code to simulate two- and three-dimensional representations of the impact events. The 2-D computations were of the penetration phase, simulating the entry, deformation and breakup of the impacting comet fragments. The calculations were performed in a "reverse ballistic" sense using a Jovian atmosphere moving upward at 60 km/s impinging upon an initially stationary fragment. The Eulerian mesh extended 100 km radially and 1000 km above and below the comet. The fragment was maintained in a high resolution portion of the mesh (equivalent to 25 computational zones across the projectile radius and extending 10 km vertically and 5 km radially) by Galilean transformations of the entire mesh every 0.1 seconds of simulation time. Zone size gradually increased away from the high resolution portion of the mesh to preserve all the materials of the calculation yet maintain computational efficiency.

The comet fragments in the simulations were composed of water ice with initial density and temperature of 0.95 g/cm^3 and 100 K, respectively, using tabularized version of the ANEOS equation-of-state which allows melting and vaporization (Thompson, 1989). The atmospheric stratigraphy in the calculations matched Voyager data for Jupiter at high altitudes (Orton, unpublished data) and extended adiabatically to lower altitudes. The atmosphere consisted of 89% hydrogen and 11% helium at all altitudes and was modeled with a tabular equation-of-state allowing dissociation and ionization (Kerley, 1991). It was scaled vertically by a factor of 1.41 (to account for the approximate 45° entry angle) and inserted into the lower portion of the computational mesh. The atmosphere propagated into the upper portion of the mesh as the comet deformed and broke up in the higher-pressure regions of the lower atmosphere.

During entry into the low density outermost reaches of the atmosphere, the projectile forms a clean bow shock. Atmospheric temperatures at the leading edge of the projectile reach values as great as 35,000 K. During deformation, the projectile thins and the leading edge flattens. Acceleration instabilities develop (Swegle and Robinson, 1989). Eventually, projectile thinning meets with the growing instabilities and breakup occurs. During penetration, the projectile continuously gives up kinetic energy to heating and deflection of the Jovian atmosphere (a relatively

small amount goes towards internal heating of the cometary constituents). Crawford et al. (1995) determined the total energy deposited by hypothetical 1-, 2- and 3-km diameter cometary fragments during their penetration of the Jovian atmosphere. An important result for fragments between 1 and 3 km in diameter was that most their kinetic energy and mass was deposited beneath Jupiter's outermost visible cloud layer, which is about 10-15 km above the reference altitude at 1-bar. Because most of the fragment's mass is deposited at depth, less than 1% is entrained in the upwardly growing fireball. Crawford et al.(1995) also investigated the influence of fragment body shape on the energy deposition profile, and tested for sensitivity to numerics by performing the same calculations with different resolutions.

The final results of the Crawford et al. (1995) fireball simulations are shown in Figure 5 for the impact of a 3-km diameter fragment. For this calculation, the results from the two-dimensional entry, deformation and breakup studies were inclined at 45° and mapped into a three-dimensional representation. Three-dimensional, bilaterally symmetric simulations most accurately rendered fireball evolution beginning about 10-15 seconds after first contact of the fragment with Jupiter's atmosphere. Density, temperature, fluid velocity and pressure of the cometary debris and shocked Jovian atmospheric constituents were preserved in a spatially average sense while total energy is conserved. The calculation was allowed to evolve for up to 120 seconds. Generally, the simulation results indicated that early-time fireball growth is predominantly directed outward along the incoming bolide trajectory but is redirected, at later time, towards growth dominated by the vertical gradient of the Jovian atmosphere. In order to attain adequate resolution for these large fireball simulations, the calculations were performed on the 1840-processor Intel Paragon massively par-
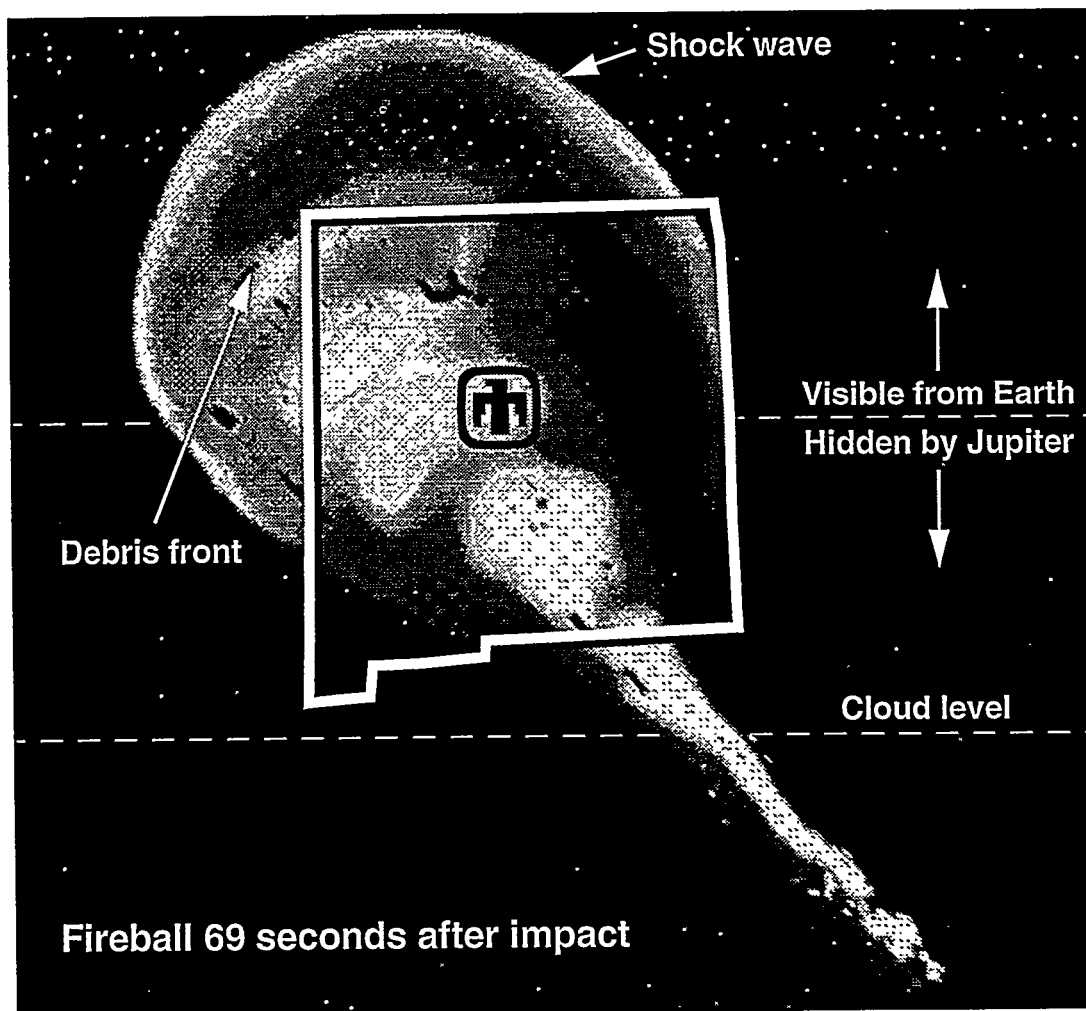

Figure 5 Cross-section of simulated fireball from the impact of a 3 km-diameter fragment of ice into Jupiter at 60 km/s, using state of New Mexico for scale. Temperature is represented by grayscale, with highest temperatures at this time step of about 2200 K (modified from Crawford et al., 1995).

allel supercomputer at Sandia National Laboratories. The simulation of the fireball formed by the impact of a 3-km comet fragment consisted of 8 million 5-km cubical zones. Lower energy events, formed by the impact of 1- or 2-km fragments, were modeled with more finely resolved, but less spatially extensive, simulations.

The fragment deposited (as internal energy of H_2, He and H_2O vapor) more than 95% of its kinetic energy (6 million megatons) during its penetration of the Jovian atmosphere (a comparatively small amount remained as kinetic energy of cometary water vapor). The fireball and surrounding shock wave resulting from a 3 km impactor is shown about 69 seconds after impact. The spherical shock wave is advancing upward at a velocity of 25 km/s. It has reached a diameter of 700 km and an altitude of 900 km above the clouds. For reference, the Jovian cloud tops are located at an altitude of 10-20 km and the limb of Jupiter (as seen from Earth) varies as a function of impact location. The limb position for impacts occurring 4 and 6 degrees beyond the limb were at 200 and 400 km altitude, respectively.

The fireball itself is a rapidly rising cloud of cometary debris and Jovian atmosphere at high temperature. Sixty-nine seconds after the impact of a 3-km cometary fragment, the fireball is still at 1700 K, and the shock wave temperature is 2300 K. An optically-thick fireball would have had an apparent bolometric magnitude (as viewed from Earth) of about 2 at this time. The observed fireballs were significantly dimmer, implying they were not optically thick.
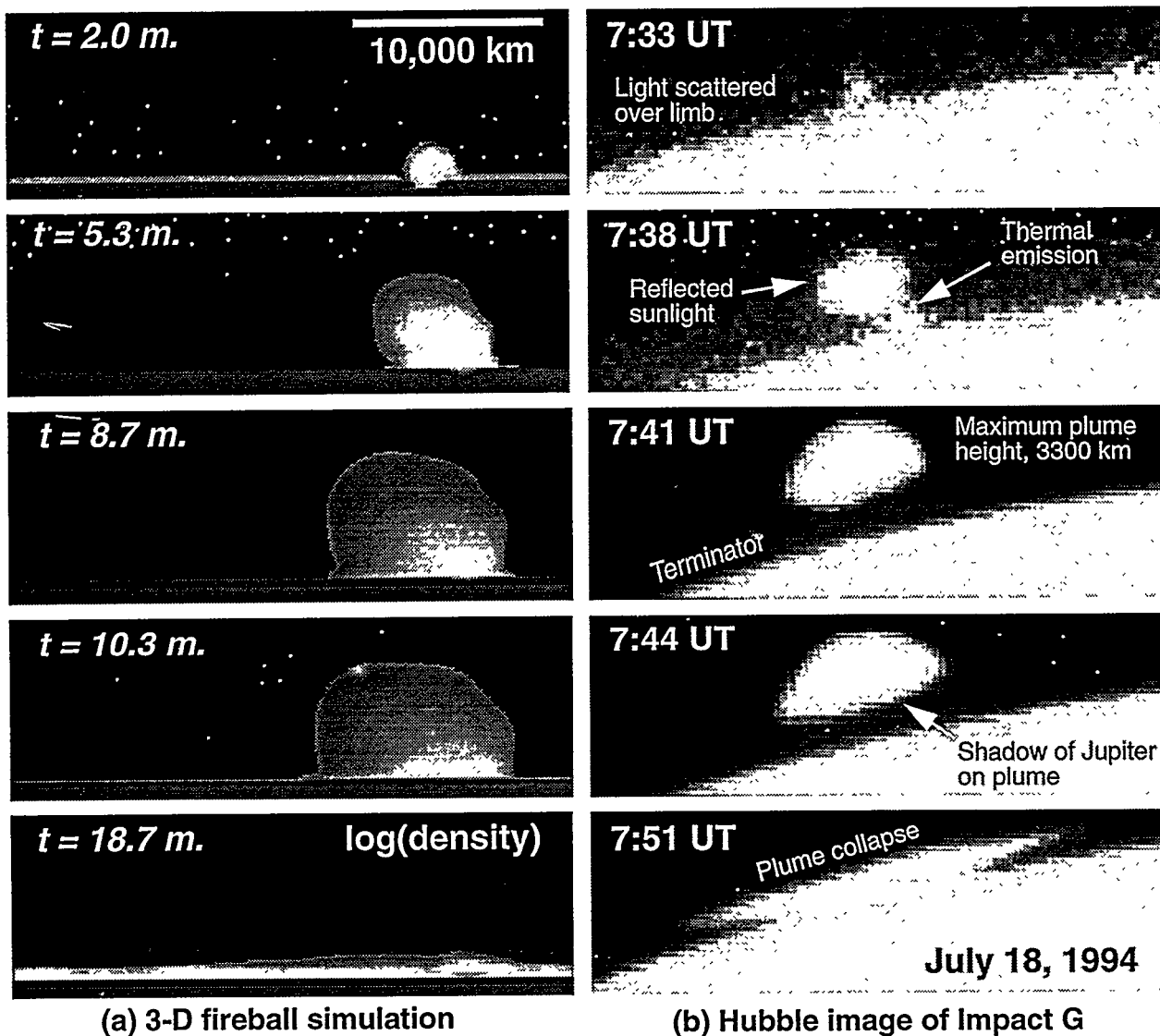

(a) 3-D fireball simulation   (b) Hubble image of Impact G

Figure 6. (a) Simulation of 3-D fireball/plume evolution after the impact of a 3-kim diameter fragment. Shading indicates log(density) with a cutoff at 10^{-12} g/cm3; times are in minutes after impact (from Crawford et al., 1995) (b) Sequence of G plume images collected by Hubble Space Telescope (from Hammel et al., 1995).

We have been calling this hot debris cloud a fireball, but the differences between it and other closely-related phenomena should be outlined. Analogies to the fireball associated with the detonation of a nuclear device are limited. The development of a nuclear fireball is dominated by interior radiative transport at temperatures of tens of millions of degrees. Some fraction of this energy forms a shock wave in the atmosphere, which separates from the fireball but can still be luminous if strong enough. The shock wave generated by the impact fireball is similar to the outer, mechanically-driven nuclear blast wave, but the temperature of the impact-generated shock wave is higher at a given propagation distance because the energy source is about six orders of magnitude greater than a megaton-scale nuclear device. The fireball itself is a ballistically-rising mixture of shocked atmosphere and vaporized cometary material. A nuclear fireball that is small compared to the scale height of the atmosphere will be driven upwards by buoyant forces because it is less dense than the surrounding atmosphere. A large impact fireball can be much greater than the scale height of the Jovian atmosphere. Because the atmospheric pressure is much greater at the bottom than at the top, it is contained at depth and relatively uncontained at altitude. It, therefore, accelerates upwards as if shot from a gun. Even though its density is much greater than the surrounding atmosphere at the top, its inertia will carry it on a ballistic trajectory which rises as much as several thousand kilometers above the clouds.

Preliminary 3-D simulations of plume evolution following the impact of a 3-km diameter ice fragment provide support for many of the interpretations presented in the previous section. Figure 6 shows that, over a period of about twenty minutes, the plume rises to its maximum height and collapses over a large area, shock-heating the upper atmosphere to temperatures on the order of 1000 K. In this simulation, the plume reaches an altitude nearly twice that observed for several plumes (including the G plume) by HST. When comparing the simulated with the observed plumes one must consider the fact that the observed plume height partially depends on the minimum density at which the debris cloud begins to condense and scatter sunlight. The diameter of the high temperature fallback region is about 30% larger than the dimensions of the G impact site. This suggests that the G fragment (or swarm of fragments) had a diameter of somewhat less than 3 km at the time of entry.

Implications for Earth-impact hazard assessment

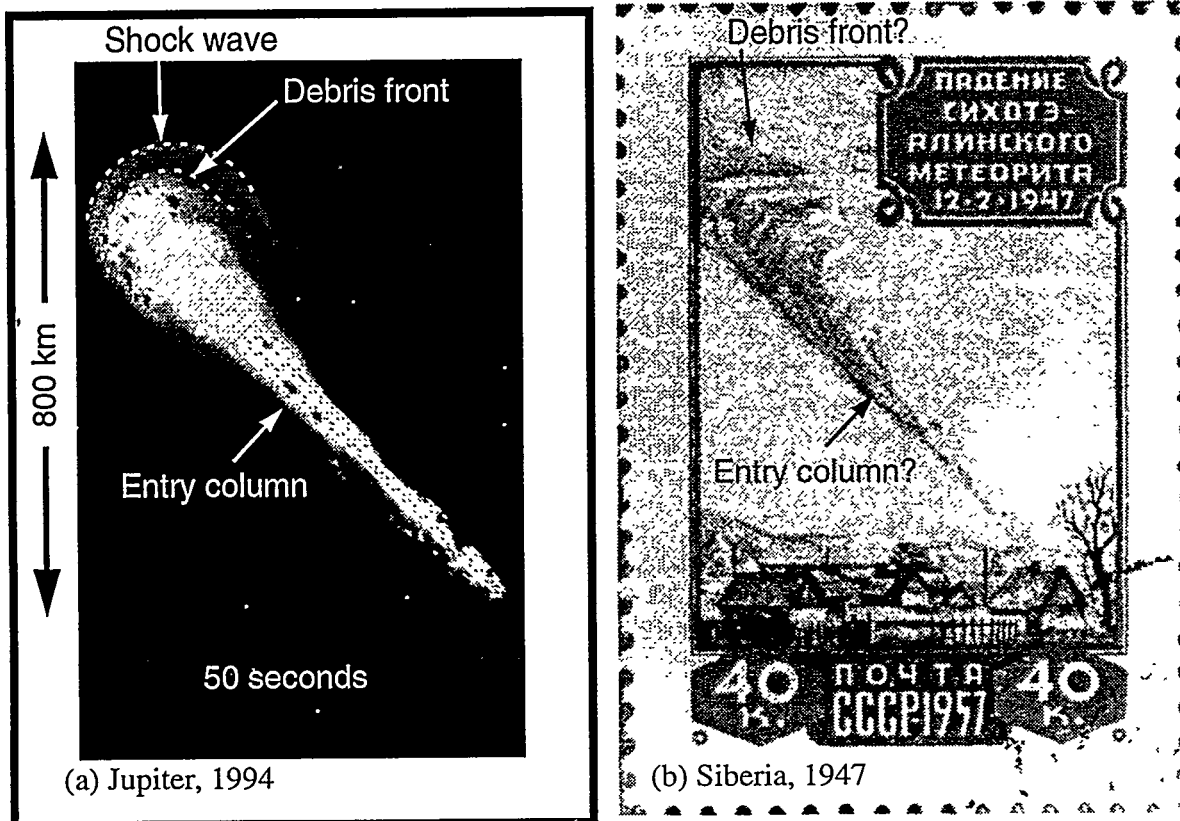Figure 7 suggests that the physics of atmospheric entry and plume generation is similar over many orders of

Figure 7 Comparison of (a) 3-D simulation of impact of 3-km diameter fragment on Jupiter, 50 seconds after entry (from Crawford et al., 1995) with (b) artist's depiction of 1947 Sikhote-Alin impact.

9

magnitude in the scale of impactor kinetic energy and physical size. The figure makes a direct comparison between the Crawford et al. (1995) 3-D fireball simulation and an eyewitness artist's depiction of the February 12, 1947 Sikhote-Alin fireball in Siberia. The Sikhote-Alin impact energy was 10-20 kilotons (Nemtchinov, 1995), whereas the simulated fireball is from a 6 million megaton impact event, nearly a billion times as energetic. The simulation image shows the explosion 50 s after the impact of a 3-km diameter fragment on Jupiter, and the illustration of the Siberian event, commemorated on a tenth-anniversary Soviet postage stamp, was recorded on canvas by artist Medvedev immediately after the fall. If the feature depicted by Medvedev represents the debris in the entry column and rising incipient plume, then its resemblance to the Jovian event implies that atmospheric impact explosions behave similarly over many orders of magnitude.

The simulations and observations of the impact of SL9 raise some issues that relate to the impact threat to Earth. In addition to demonstrating that objects do indeed collide with planets, the series of impacts has shown that ballistic impact fireballs and plumes are ejected to very high altitudes, and that explosive expansion of shocked atmosphere along the entry column is highly directional and poorly modeled by point explosions. These observations lead to the suggestion that satellites in low-Earth orbit (LEO) may be vulnerable to ejection of material into their environment by an impact into the atmosphere. Because of the high orbital velocities of these satellites (about 7 km/s), even a very low-density plume ejected into their path would be catastrophic. For a vapor plume, a satellite/plume interaction would be similar to an atmospheric reentry. At best, an interaction with a very low-density plume would cause a change in the attitude and orbit of the satellite. A worse outcome would result from a higher-density plume, which could cause premature reentry or otherwise destroy the satellite. For a plume containing particles of condensation, like those generated by SL9, the interaction would involve numerous hypervelocity impacts similar to those occasionally experienced with space debris and micrometeorites. This would most likely end the life of the satellite.
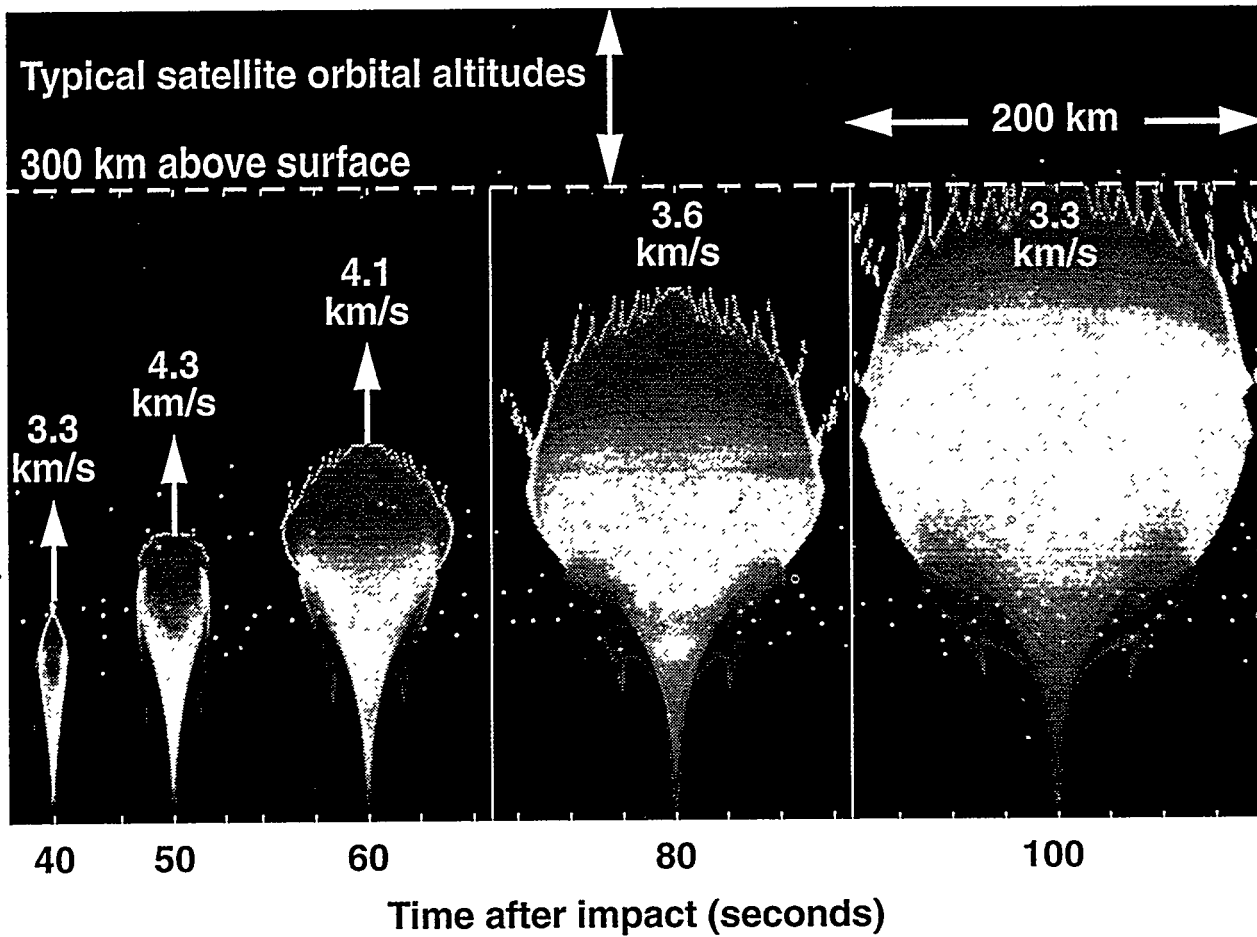
Computational modeling of Earth-impact plumes

To test this idea, we have performed preliminary 2-D simulations of the plume generated by a 34-m diameter stone (density=3 g/cm^3) impacting at 20 km/s with vertical incidence. The kinetic energy of the impactor is equivalent to an explosive yield of 3 Megatons of TNT, and the expected frequency of such an event is about once per century (Morrison et al., 1995). The simulation was performed using the CTH shock physics code (McGlaun et al., 1990) by inserting an appropriate impact energy deposition curve into a gravitationally-stabilized, stratified Earth atmosphere, using the 1976 U.S. Standard Atmosphere (NOAA, NASA, USAF, Washington D.C., 1976) density profile. The energy deposition curve was calculated using the model of Crawford (1995) which assumes negligible radiative ablation for 10+ m objects in Earth's atmosphere (as required by momentum conservation) and hydrodynamic deformation governed by long-wavelength Kelvin-Helmholtz instability. This model has been calibrated with results of entry simulations using CTH.

The energy was inserted as 100 discrete energy sources with appropriate magnitudes along the axis of symmetry from 120 km to the surface. The individual "point charges" were set off sequentially, beginning at the top, and initiating downward with the velocity of the projectile, accounting for its deceleration as it descends into the atmosphere. This method of energy insertion effectively simulates the entry column as a line charge of varying energy density.

A time sequence showing the results of the simulation is given in Fig. 8(a). The shading indicates material velocity magnitudes, ranging from 100 m/s to 3 km/s. Immediately after entry, the meteoroid has deposited its energy in a long column, with a sharp peak in the energy deposition curve at an altitude of 7 km. The column begins to expand explosively the instant that energy is deposited in the column, so by the time the object reaches the bottom, the top of the column has had time to expand and accelerate upwards. When the main fireball begins to develop lower down, it expands most easily up along the low-density, high-sound-speed column that is already moving upward. In this way, much of it's mass is accelerated and launched into space as a "ballistic fireball". At about 100 seconds after atmospheric entry, the top of the plume (as defined by the 120 km density contour) has reached an altitude of nearly 300 km, and is still moving upward at a velocity of about 3 km/s (the "fingers" protruding from the top of the plume are an artifact of numerical instabilities resulting from the relatively low resolution used for this simulation). Ballistic extrapolation indicates a peak plume height at about 800 km, putting it across the path of many satellites in LEO. The plume will have a "hang time" greater than 10 minutes; during this interval it will obstruct any satellite passing overhead. Furthermore, it will continue to expand radially during this time to cover a region thousands of kilometers in diameter. Observations and simulations of the plume collapse on Jupiter imply that the atmospheric density contours in the region of collapse will remain elevated for a much longer period of time, posing a further risk to satellites entering the area.

(a) 3 MT impact source produces high velocity "ballistic fireball"

Typical satellite orbital altitudes

300 km above surface

←— 200 km —→

3.6 km/s

3.3 km/s

4.1 km/s

4.3 km/s

3.3 km/s

40   50   60   80   100

Time after impact (seconds)

(b) 3 MT explosion source produces low velocity "buoyant fireball"

420 m/s   400 m/s   360 m/s   310 m/s   225 m/s

100 km

40   50   60   80   100

Time after explosion (seconds)
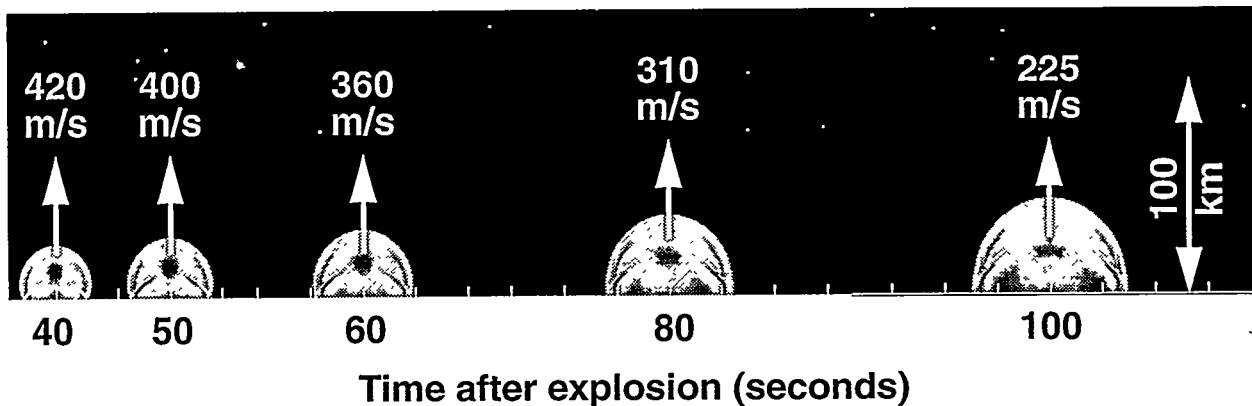
Figure 8. Comparison on the same scale of evolution of (a) ballistic fireball generated by 3 megaton impact to (b) buoyant fireball generated by a 3 megaton explosion at same altitude of maximum energy deposition (7 km). Shading indicates velocity magnitude of the air as indicated in the text.

11

For comparison, we simulated a point source explosion of 3 MT in the same Earth atmosphere. We kept all other conditions identical and inserted a single energy source at an altitude of 7 km, the point of maximum energy deposition for the entry calculation. Figure 8(b) shows that no plume has formed by 100 s after the start of the calculation, suggesting that the point explosion is well-tamped by the overlying atmosphere, and more realistic linear energy sources are much more efficient at generating plumes. The upward velocity of the fireball is lower by an order of magnitude, and it was necessary to redefine the velocity shading scale in order to see it in these plots (shading ranges logarithmically from 0.5 to 400 m/s). The mass motion in this case is dominated by density, and results in a "buoyant fireball" typical of free-air burst nuclear explosions.

Observational validation

The impact of SL9 underscores the importance of observational validation of impact modeling. It is probably not realistic to expect another opportunity to watch a comet collide with Jupiter, an event that probably only happens once in a period ranging from 200 to 10,00 years (Shoemaker, 1995). A more reasonable plan would be to attempt to gather as much information as possible about the smaller atmospheric impacts that are continuously taking place on Earth. If the physics of atmospheric entry and plume formation indeed scales well over 9 orders of magnitude, then careful, quantitative measurements of impacts that take place at intervals of a year or less would give entry and impact models the degree of validity necessary to allow their use as a basis for hazard assessment. To accomplish this task, we recommend a coordinated campaign based on a combination of satellite sensors and Earth-based observations. Infrared and visible-light sensors on satellites operated by the U.S. Department of Defense have already detected over a hundred events (Tagliaferri et al., 1995), including the February 1, 1994 bolide over the South Pacific with an estimated energy of 40-70 kilotons (Nemchinov, 1994). Microbarograph records are particularly useful in characterizing the explosive yield of large impact events, and have recorded an explosion as large as 1.1 megatons for the October 3, 1963 bolide over the ocean south of Africa (Revelle, 1995). Other sources of data that can be used to validate the simulations are photographic and video images (e.g. Ceplecha, 1994; Brown et al., 1994), and seismic data.

There is one major drawback in all the above methods as they have been used to date: the events they observed were not predicted in advance. Therefore, the instrumentation was operated in "open shutter" mode, or set to trigger off of the event, or relied on serendipity. By contrast, the impact of SL9 was predicted a year in advance, and observing plans were carefully assembled well in advance of the event, resulting in the collection of vast amounts of high-quality data. We suggest a similar strategy would be most useful for validation of Earth impact models. A ground-based search system capable of providing short notice of an impact in the 100 kiloton range would mean that the approaching object could be characterized before impact. Moreover, arrays of sensors, cameras, and satellite observing plans to be quickly put in place so that data from the event could be captured and used to provide quantitative validation.

Conclusions

Preliminary computational analysis suggests that satellites at low altitude are at significant risk from plumes due to impacts as small as a few megatons. This conclusion is based on the insight, physical understanding, and model validation gained from observations of the impact of comet Shoemaker-Levy 9. This newly-recognized threat should be examined by further modeling and by extensive observational validation by gathering data on the continuous impact flux of smaller objects.

Acknowledgments

References

Ahrens, T. J., Takata, T., O'Keefe, J. D., and Orton, G. S., "Radiative Signatures from Impact of Comet Shoemaker-Levy 9 on Jupiter," *Geophys. Res. Lett.*, 21(14), 1551-1553, 1994.

Boslough, M. B., Crawford, D. A., Robinson, A. C., and Trucano, T. G., "Mass and Penetration Depth of Shoemaker-Levy 9 Fragments from Time-Resolved Photometry, *Geophys. Res. Lett.*, 21(14), 1555-1558, 1994a.

Boslough, M. B., Crawford, D. A., Robinson, A. C., and Trucano, T. G., "Watching for Fireballs on Jupiter," *Eos*, 75(27), 305-310, 1994b.

Boslough, M. B., Crawford, D. A., Trucano, T. G., and Robinson, A. C., "Numerical Modeling of Shoemaker-Levy 9 Impacts as a Framework for Interpreting Observations," *Geophys. Res. Lett.*, 22(13), 1821-1824, 1995.

Brown, P., Ceplecha, Z., Hawkes, R. L., Wetherill, G., Beech, M., and Mossman, K., "The Orbit and Atmospheric Trajectory of the Peekskill Meteorite from Video Records," *Nature*, 367, 624-626, 1994.

Carlson, R. W., Weissman, P. R., Segura, M., and the NIMS Science Team, "Galileo Infrared Observations of the Shoemaker-Levy 9 G Impact Fireball: A Preliminary Report," *Geophys. Res. Lett.*, 22(12), 1557-1560, 1995.

Ceplecha, Z., "Earth-Grazing Daylight Fireball of August 10, 1972," *Astron. Astrophys.*, 283, 287-288, 1994.

Chapman, C. R., Merline, W. J., Klaasen, K., and the Galileo Imaging Team, "Preliminary Results of Galileo Direct Imaging of S-L 9 Impacts," *Geophys. Res. Lett.*, 22(13), 1561-1564, 1995.

Crawford, D. A., "Models of Fragment Penetration and Fireball Evolution," in *The Collision of Comet Shoemaker-Levy 9 with Jupiter*, K. Noll, editor, in press, 1995.

Crawford, D. A., Boslough, M. B., Trucano, T. G., and Robinson, A. C., "The Impact of Comet Shoemaker-Levy 9 on Jupiter," *Shock Waves*, 4(1), 47-50, 1994.

Crawford, D. A., Boslough, M. B., Robinson, A. C., and Trucano, T. G., "Dependence of Shoemaker-Levy 9 Impact Fireball Evolution on Fragment Size and Mass," *Lunar and Planetary Science* XXVI, 291-292, 1995.

Crawford, D. A., Boslough, M. B., Trucano, T. G., and Robinson, A. C., The impact of periodic comet Shoemaker-Levy 9 on Jupiter, *Int. J. Impact. Engng.*, in press, 1995.

Graham, J. R., de Pater, I., Jernigan, J. G., Liu, M. C., and Brown, M. E., "The Fragment R Collision: W. M. Keck Telescope Observations of SL9," *Science*, 267, 1320-1323, 1995.

Hammel, H. B., Beebe, R. F., Ingersoll, A. P., and 14 others, "HST Imaging of Atmospheric Phenomena Created by the Impact of Comet Shoemaker-Levy 9," *Science*, 267, 1288-1296, 1995.

Hord, C. W., Pryor, W. R., Stewart, A. I. F., and 10 others, "Direct Observations of the Comet Shoemaker-Levy 9 Fragment G Impact by Galileo UVS," *Geophys. Res. Lett.*, 22(13), 1565-1568, 1995.

Kerley, G. I., "User's Manual for PANDA II: A Computer Code for Calculating Equations of State," Sandia National Laboratories, SAND88-2291, 1991.

Livengood, T. A., Bjoraker, G., Kostiuk, T., and 6 others, *Bull. Am. astr. Soc.*, 26, supplement, 1994.

Maillard, J.-P., Drossart, P., Bezard, B., and 6 others, "Methane and Carbon Monoxide Infrared Emissions Observed at the Canada-France-Hawaii Telescope During the Collision of Comet SL-9 with Jupiter," *Geophys. Res. Lett.*, , 22(12), 1573-1576, 1995.

Marten, A., Gautier, D., Griffen, M.J., and 14 others, "The Collision of Comet Shoemaker-Levy 9 with Jupiter: Detection and Evolution of HCN in the Stratosphere of the Planet," *Geophys. Res. Lett.*, 22(12), 1589-1592, 1995.

Martin, T. Z., Orton, G. S., Travis, L. D., Tamppari, L. K., and Claypool, I., "Observation of Shoemaker-Levy Impacts by the Galileo Photopolarimeter Radiometer," *Science*, 268, 1875-1878, 1995.

McGlaun, J. M., Thompson, S. L., and Elrick, M. G., "CTH: A Three Dimensional Shock-Wave Physics Code," *Int. J. Impact. Engng.*, 10, 351, 1990.

Morrison, D., Chapman, C. R., and Slovic, P., "The Impact Hazard," in *Hazards Due to Comets and Asteroids*, T. Gehrels, ed., U. Arizona Press, Tucson, 1995.

Nemchinov, I. V., "Assessment of the 1 February 1994 Event," Interim report 006 to Sandia National Laboratories, 1994.

Nemchinov, I. V., "Analysis of the 12 February 1947 Event," Interim report 01A to Sandia National Laboratories, 1995.

Nicholson, P. D.,Gierasch, P., Hayward, and 10 others, "Palomar Observations of the R Impact of Comet Shoemaker-Levy 9: I. Light Curves," *Geophys. Res. Lett.*, 22(12), 1589-1592, 1995.

Revelle, D. O., "Historical Detection of Atmospheric Impacts by Large Bolides Using Acoustic-Gravity Waves," International Conference on Near-Earth Objects, New York, April 24-26, 1995.

Roos-Serote, M., Barucci, A., Crovisier, J., Drossart, P., Fulchignoni, M., Lecacheux, J., and Roques, F., "Metallic Emission Lines During the Impacts L and Q_1 of Comet P/Shoemaker Levy 9 in Jupiter," *Geophys. Res. Lett.*, 22(12), 1621-1624, 1995.

Shoemaker, E. M., "Comet Shoemaker-Levy 9 at Jupiter,", *Geophys. Res. Lett.*, 22(12), 1555-1556, 1995.

Shoemaker, E. M., Hassig, P. J., and Roddy, D. J., "Numerical Simulations of the Shoemaker-Levy 9 Impact Plumes and Clouds: A Progress Report, *Geophys. Res. Lett.*, 22(13), 1825-1828, 1995.

Stellingwerf, R. F., Hoffman, N. M., and Wingate, C. A., *Bull. Am. astr. Soc.*, 26, 880, 1994.

Swegle, J. W., and Robinson, A. C., "Acceleration Instability in Elastic-Plastic Solid. I. Numerical Simulations of Plate Acceleration," *J. Appl. Phys.*, 66, 2838, 1989.

Tagliaferri, E., Spalding, R., Jacobs, C., Worden, P., and Erlich, A., "Detection of Meteoroid Impacts by Optical Sensors in Earth Orbit," in *Hazards Due to Comets and Asteroids*, T. Gehrels, ed., U. Arizona Press, Tucson, 1995.

Takeuchi, S., Hasegawa, H., Watanabe, J., and 5 others, "Near-IR Imaging Observations of the Cometary Impact Into Jupiter," *Geophys. Res. Lett.*, 22(12), 1581-1584, 1995.

Thompson, S. L., "ANEOS Analytic Equations of State for Shock Physics Codes Input Manual," Sandia National Laboratories, SAND89-2951, 1989.

Zahnle, K., and Mac Low, M.-M., "The Collision of Jupiter and Comet Shoemaker-Levy-9," *Icarus*, 108, 1-17, 1994.

DISCLAIMER